

IOP Conference Series: Materials Science and Engineering

PAPER • **OPEN ACCESS**

Fractal characterization of conductive Ag/flexible 3D printed PLA

To cite this article: F.M. Mwema *et al* 2021 *IOP Conf. Ser.: Mater. Sci. Eng.* **1107** 012050

View the [article online](#) for updates and enhancements.



 **The Electrochemical Society**
Advancing solid state & electrochemical science & technology

 **18th**

239th ECS Meeting with IMCS18

DIGITAL MEETING • May 30-June 3, 2021

Live events daily • Free to register

[Register now!](#)

The banner features a background image of a person's head with a network of lines and nodes, symbolizing digital connectivity. The ECS logo is on the left, and the IMCS18 logo is on the right. A red button with the text 'Register now!' is at the bottom right.

Fractal characterization of conductive Ag/flexible 3D printed PLA

F.M. Mwema^{1,2*}, A.A. Adediran^{3,4}, E.T. Akinlabi², A.A. Adeleke³ and T.M.A. Olayanju⁴

¹Materials, Design and Manufacturing (MADEM) Group, Department of Mechanical Engineering, Dedan Kimathi University of Technology, 10143, Nyeri, Kenya.

²Mechanical Engineering Department, University of Johannesburg, South Africa.

³Department of Mechanical Engineering, Landmark University, PMB 1001, Omu-Aran, Kwara State, Nigeria.

⁴Landmark University Waste to Wealth Energy Initiative (LUWWEI), PMB 1001, Omu-Aran, Kwara State, Nigeria.

Corresponding

Author;

fredrick.mwema@dkut.ac.ke,

adediran.adeolu@lmu.edu.ng, +254 723 015709

Abstract-

In this paper, thin and flexible PLA plates were prepared through FDM printing process. The traditional FDM process was adopted at predetermined optimal printing parameters of the 3D printer. The CAD designs of the samples were built on SpaceClaim modeler (ANSYS® 2019). The slicing and generation of the toolpath (gcodes) were undertaken in Cura software whereas the printing undertaken using a Desktop 3D printer (WANHAO Duplicator D10). The flexible PLA samples were designed for conductivity in smart devices; as such, they were coated with micro-films of highly conductive silver paint through a dipping method. The dipping was carefully undertaken in which the samples could soak inside the paint for 40 seconds and then removed and allowed to dry in vacuum desiccators for 12 hours. The samples were then heat treated at varying times (0, 10 and 20 minutes) in an oven at a constant temperature of 100°. The samples were then profiled using atomic force microscopy to obtain the microroughness characteristics of the Ag/PLA surfaces. The height features as well as spatial roughness characteristics were obtained through mono-fractal and multifractal approaches. The influence of heat treatment times at the reported temperature is shown to significantly influence the spatial roughness characteristics of the 3D printed flexible samples.

Key words: Cocoa beans, marketing risk factor, plant layout

1. Introduction

Additive manufacturing (AM)/3D printing is a very exciting technology in the modern industry due to its flexibility. Of the AM methods, fused deposition modelling (FDM), which mostly utilizes polymeric raw materials is mostly due to its ease in use and affordability. The FDM technology is widely used in rapid prototyping, model generation and manufacturing of functional parts [1–3]. The technology is very attractive for fabrication of flexible conductors for applications in smart devices and microelectronics [4]. To achieve conductivity in such materials, two methods can be chosen (i) metallization of the 3D printed polymer or (ii) use of conductive polymeric filaments such as graphene-doped PLA [5–7]. Using conductive filaments appears to be the easiest procedure, however, it requires special or advanced 3D printing machine since it has difficulties of adhering onto the build plate. Since most desktop and low-cost printers do not have heated bed functionality, it is difficult to produce such



products. As such, the metallization of the printed (flexible) substrates is the alternative to such 3D printer users. There are several technologies for metallization of printed substrates ranging from basic dipping method to advanced chemical/physical vapor deposition techniques [8, 9]. In this work, we illustrate, for the first time, the use of atomic force microscope (AFM) in studying the fractal characteristics of Ag/PLA 3D printed samples for flexible conductors. The 3D printed PLA substrate (flexible) was coated using a high conductive silver paint through a dipping method. The coated samples were then heat treated for different times at constant oven temperature.

2. Experimental Methods

In this work, polylactic acid (PLA) rectangular and flexible strips were prepared through fused deposition modelling using a desktop (home) 3D printer. A WANHAO D10 Duplicator 3D printer model was used at printing speed of 50 mm/s, layer thickness of 0.1 mm and print orientation of 0°. The printing was undertaken on a non-heated bed using brim without any support. Further details of the 3D printer and parameters can be found in our previous article [10]. The 3D printed samples were then coated using a thin layer of conductive silver paste through a dipping process. The commercial silver paint was purchased from RS components, Johannesburg, South Africa. The coated samples were then allowed to dry in atmosphere for 24 hours before being heat treated in an oven. The heat treatment was undertaken at a constant temperature of 100°C but at varying exposure times of 0, 10 and 20 minutes. The 0-minute sample in this case means that the sample was not heat treated. The surfaces of the coated samples were then characterized via atomic force microscopy (AFM) and scanning electron microscopy (SEM). The AFM micrographs were further exported to an image analyses procedure to undertake fractal characterization according to established literatures [11–14].

3. Results and discussion

Figures 1, 2 and 3 shows the AFM images of the silver coated samples without heat treatment, heat treated for 10 and 20 minutes respectively. As shown, both 2D and 3D height maps are presented. The sample without heat treatment is shown to exhibit sharp and larger surface features, which contributes to higher surface roughness as shown in Figure 4. On heat treatment, there is flow of the PLA material, which causes efficient interaction between the substrate (PLA) and silver coating. As such, the heat-treated samples exhibit fewer surface defects and hence lower surface roughness values (Figure 4). An average computed fractal dimensions on the surfaces of the samples does not reveal any significant variation with heat treatment. After 20 minutes, the surface structures. This implies that the heat treatment has insignificant influence on the lateral roughness at the surface of these samples.

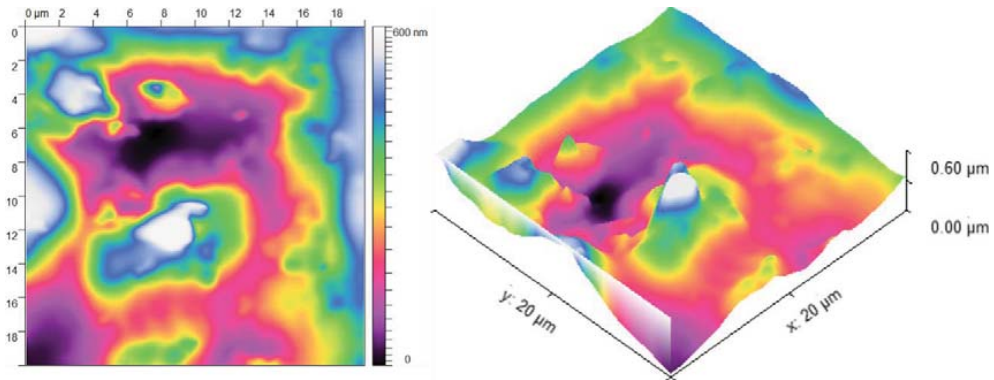


Figure 1: Atomic force microscopy images for the Ag/PLA samples before heat treatment

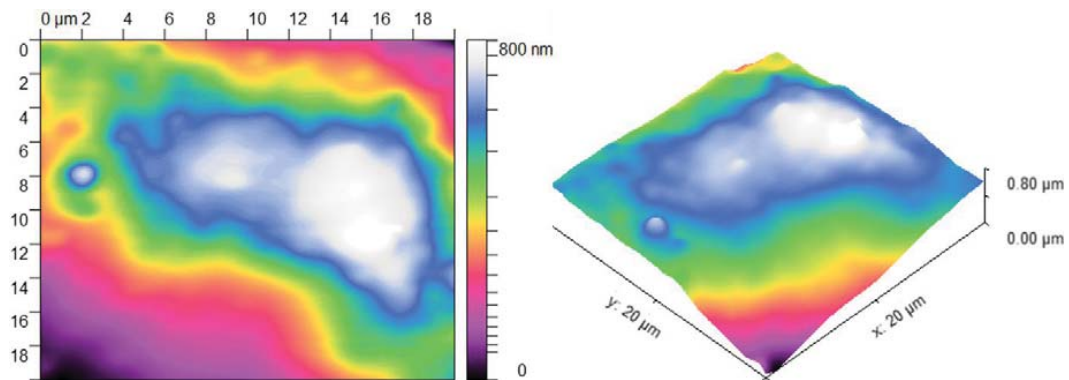


Figure 2: Atomic force microscopy images for the Ag/PLA samples on heat treatment for 10 minutes

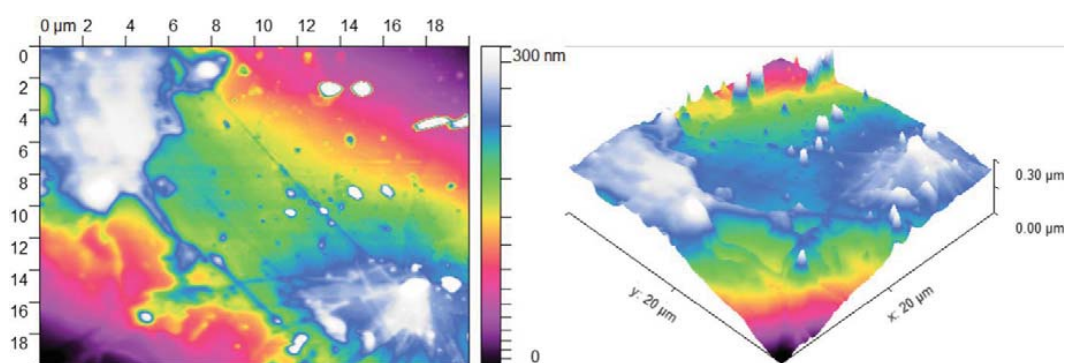


Figure 3: Atomic force microscopy images for the Ag/PLA samples on heat treatment for 20 minutes

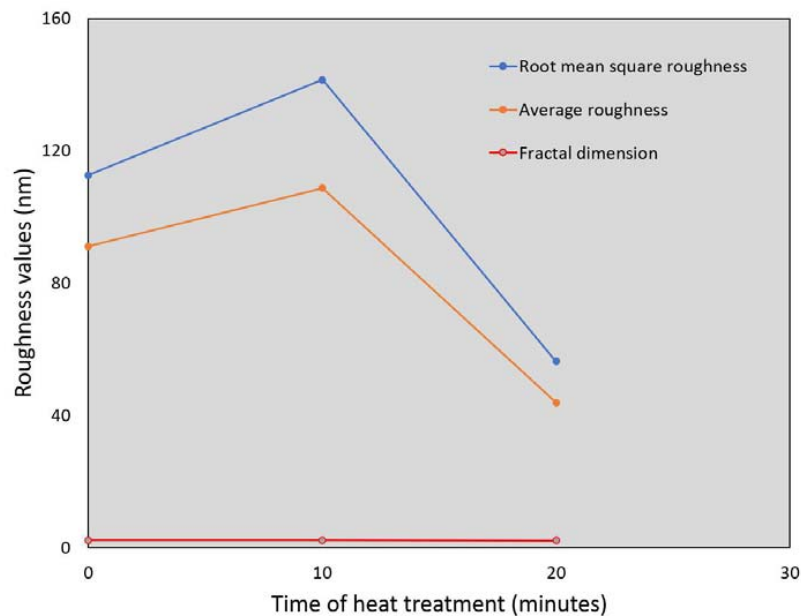


Figure 4: The variation of roughness values and fractal dimensions with the time of heat treatment

Further image analyses were undertaken to determine more fractal behaviour of the Ag/PLA samples. Specifically, results on height-to-height functions (HHCF), power spectral density functions (PSD) and 2D Minkowski functionals were generated and are presented in Figures 5, 6, and 7 respectively. Theoretical representations of these functions are readily available in literature as [15–19]. As shown in Figure 5, the HHCF bi-logarithmic plots exhibit two regions; (i) linear and (ii) nonlinear regions at small and large values of r respectively. Such plots are characteristic of self-affine surfaces and similar behaviour has been reported for physically deposited thin films [12, 20]. It can be seen that the transition between the two regimes fades (becomes indistinct) as the heat treatment time increases from 0 to 20 minutes. This implies that the fractal behaviour of non-heat-treated samples can be determined by both power law and Gaussian functions whereas for samples heat treated for 20 minutes can be approximated using only a power law function.

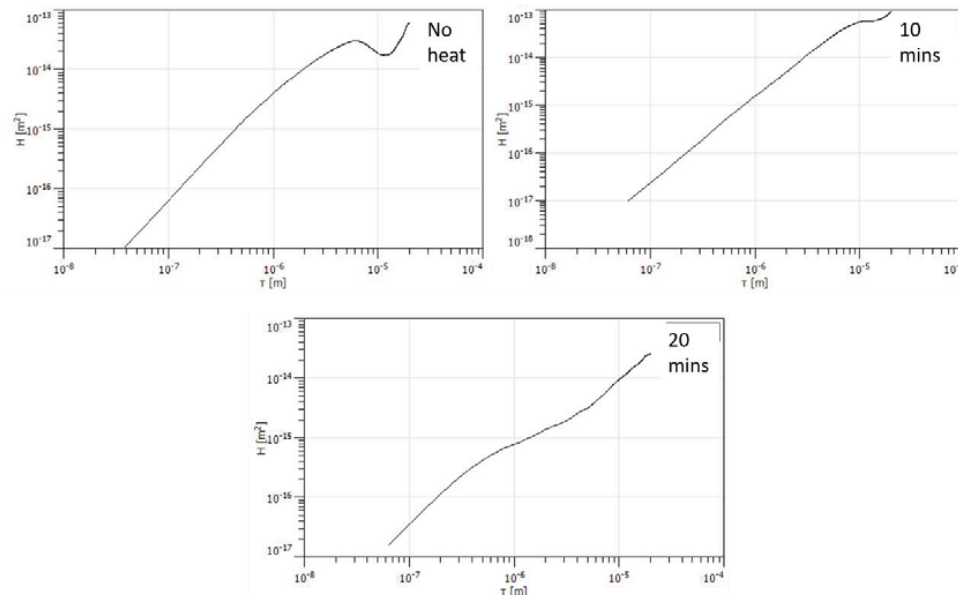


Figure 5: Bi-logarithmic plots of height-height correlation functions as a function of shift (r) for the Ag/PLA surfaces at different heat treatment conditions

A further analysis of the fractal behaviour of the 3D printed samples of Ag/PLA was undertaken through power spectral density functions (PSD) and a log-log representation of the results are shown in Figure 6.

As shown, the plots exhibit two regions, namely, a white noise region and power law region. The white noise region is usually a flat section of the PSD function and occurs mostly at low spatial frequency whereas the highly correlated region occurs at high spatial frequency of the power spectrum. A larger white noise region is an indication of existence of non-variational surface features and in this work, it indicates presence of pure surfaces of either PLA or Ag. The white noise region is seen to decrease with increase in heat treatment time. This indicates that heat treatment helps in homogenization of the surface structure. Additionally, the highly correlated region indicates the presence of well-defined surface features due to the heat treatment, which enhances the ‘mixing’ of the PLA and Ag structures. After 20 minutes of heat treatment, the PSD plot is a highly correlated function which can easily be described by a power law. According to these results, heat treatment enhances homogenous interaction between the thin coating of Ag and substrate PLA.

The Minskowski functionals shown in Figure 7 are used to indicate the morphological features that cannot be determined through classical methods. There are three parameters presented, namely, the boundary length (S), connectivity (X) and volume (V). These parameters are based on separating the high and low resolutions in a micrograph. As shown, these functionals vary with the heat treatment, indicating the structural transformations at the surface of the Ag/PLA samples towards homogeneity. For instance, the X values tend to positive dominance as the time of heat treatment increases. This indicates that the surface structures are homogeneous and have close structural characteristics. Additionally, the S functionals tend to become asymmetrical as the heat treatment time increases. There were no major variations in V parameters as the heat treatment time increased from 10 to 20 minutes although a

considerable change can be observed from 0 to 10 minutes of heat treatment. This can be a subject of future research as it may require further theoretical approach which is not an objective of this paper.

Figure 8 shows high resolution SEM images obtained on the Ag/PLA cross-sections and at the surfaces of the samples to observe the Ag and PLA interactions and structural evolution. A clear distinction between the film and substrate is observed on the non-heat-treated samples whereas the interface appears continuous for the heat-treated samples. This indicates that heat treatment enhances flow of the PLA allowing adhesion of the Ag coating onto its structure. Furthermore, at the top surface of the heat-treated samples, very fine and well-defined structures of the Ag in the PLA matrix can be observed.

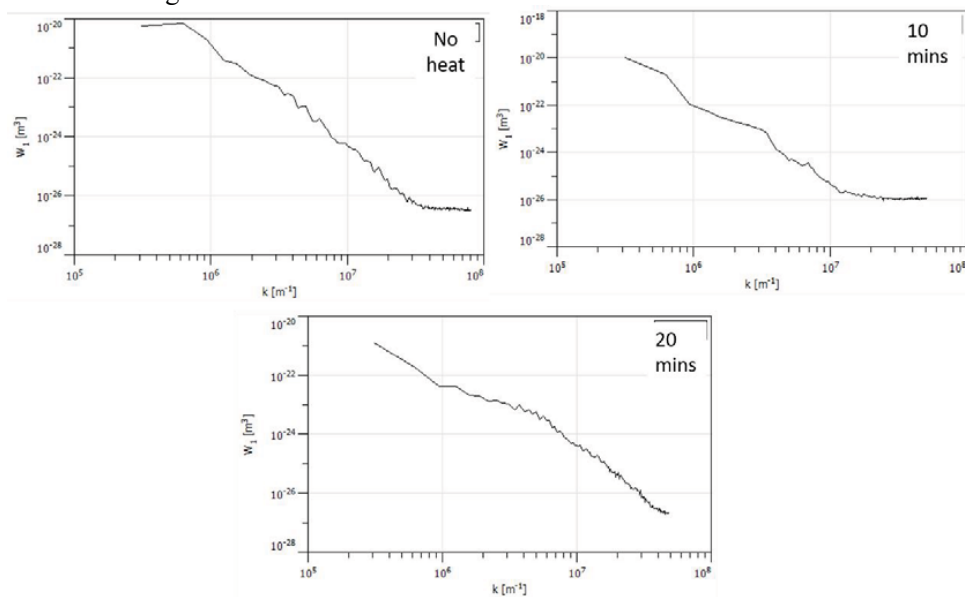


Figure 6: Power spectral density (PSD) functions of the 3D printed Ag/PLA samples exposed to heat treatment at different times

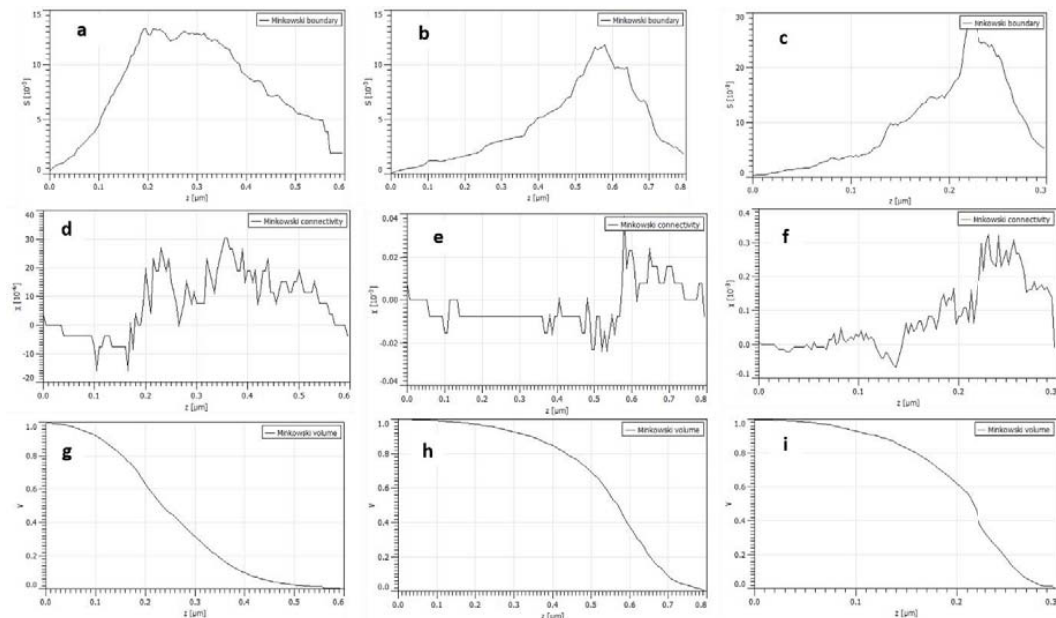


Figure 7: Minkowski functionals for the Ag/PLA 3D printed samples at non-heat-treated (a, d, g), heat treated for 10 minutes (b, e, h) and 20 minutes (c, f, i): (a)-(c) Boundary length (S), (d)-(f) Connectivity, (X) and (g)-(i) volume (V)

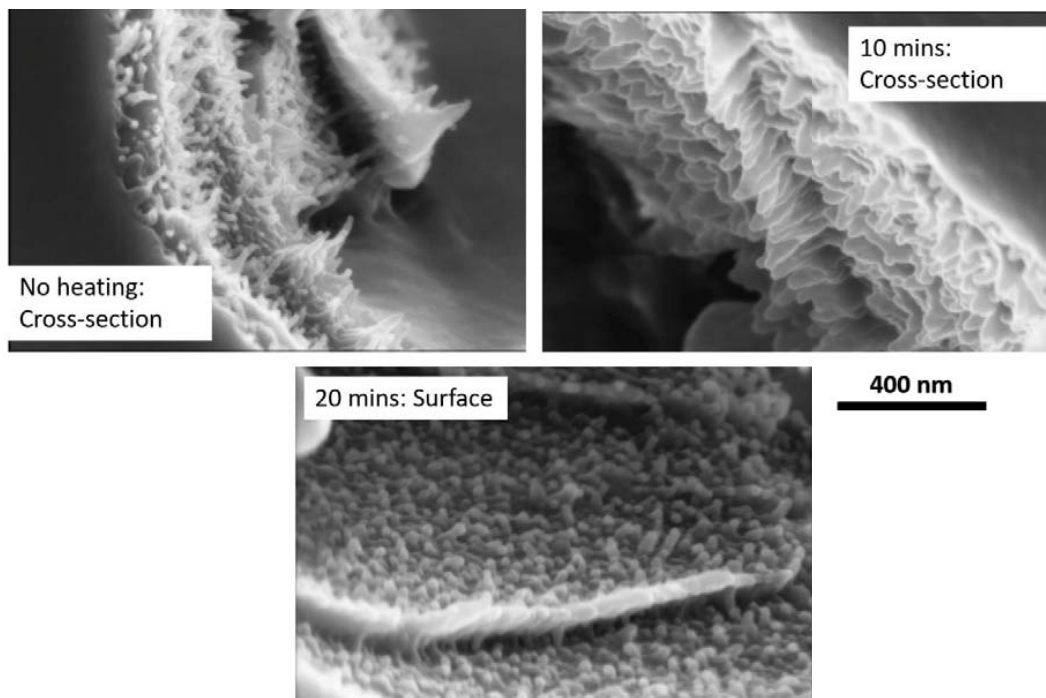


Figure 8: Scanning electron microscope of the 3D printed Ag/PLA in non-heat-treated and heat-treated conditions

4. Conclusions

In this article, 3D printed PLA substrates were coated using Ag paint through dipping method and microstructural and fractal analyses undertaken. The following important conclusions can be deduced from the study:

- ❖ Heat treatment causes a phenomenon analogous to flow-softening on 3D printed PLA substrate, which further flows leading to homogeneous interaction with the Ag coating.
- ❖ 3D printed Ag/PLA samples exhibit self-affine characteristics and can be described via known fractal theories such as height-height correction, power spectral density, Minskowski functionals.
- ❖ The fractal behaviour of Ag/PLA samples vary with heat treatment, indicating that there occurs both vertical and lateral transformation and interaction between the substrate and coating on heat treatment.
- ❖ Heat treatment enhances adhesion of the Ag film onto the PLA and refinement of the Ag structure.

Despite these observations, there are questions arising that will require further research:

- ❖ The mechanism of formation of well-defined structure of the Ag onto the PLA structure.
- ❖ The variation of Minskowski functionals with heat treatment is not exhaustive and further theoretical approach using simulated surface topography is recommended for comprehensive study into the phenomenon.

Acknowledgements

The GES 4.0 postdoctoral fellowship (2019/2020) of the University of Johannesburg is highly acknowledged. Dr. Dinara Sobola of the Brno University of Technology, Brno, Czech Republic is highly acknowledged for her assistance on high resolution SEM and Joan Nyika, A PhD research at UNISA is acknowledged for her help on heat treatment of the Ag/PLA samples. A.A.A. appreciates Landmark University Centre for Innovation, Research, and Development (LUCRID) for their support.

References

- [1] Dey, A. & Yodo, N. (2019). A systematic survey of FDM process parameter optimization and their influence on part characteristics. *Journal of Manufacturing & Materials Processing*, 3(3), 64.
- [2] McCullough, E. J. & Yadavalli, V. K. (2013). Surface modification of fused deposition modeling ABS to enable rapid prototyping of biomedical micro devices, *Journal of Materials Processing Technology*, 213(6), 947–954.
- [3] Hamzah, H. H., Shafiee, S. A., Abdalla, A., & Patel, B. A. (2018). 3D printable conductive materials for the fabrication of electrochemical sensors: A mini review, *Electrochemistry Communications*, 96, 27–31.
- [4] White, J. Tenore, C. Pavich, A. Scherzer, R. & Stagon, S. (2018). Environmentally benign metallization of material extrusion technology 3D printed acrylonitrile butadiene styrene parts using physical vapor deposition, *Additive Manufacturing*, 22, 279–285.
- [5] Saxena, P. & Metkar, R. M. (2019). Development of Electrical Discharge Machining

- (EDM) Electrode using Fused Deposition Modeling (FDM), in 3D Printing and Additive Manufacturing Technologies, Singapore: Springer Singapore, 257–268.
- [6] Kim, M. J., Cruz, M.A., Ye, S., Gray, A.L., Smith, G.L., Lazarus, N., Walker, C.J., Sigmarsson, H.H., & Wiley, B.J. (2018). One-step electrodeposition of copper on conductive 3D printed objects, *Additive Manufacturing*, 27, 318–326.
 - [7] Katseli, V., Economou, A. & Kokkinos, C. (2019). Single-step fabrication of an integrated 3D-printed device for electrochemical sensing applications, *Electrochemistry Communications*, 103, 100–103.
 - [8] Lee, K.-M., Park, H., Kim, J., & Chun, D.-M. (2018). Fabrication of a superhydrophobic surface using a fused deposition modeling (FDM) 3D printer with poly lactic acid (PLA) filament and dip coating with silica nanoparticles, *Applied Surface Science*, 467–468, 979–991.
 - [9] Haidiezul, A. H. M., Aiman, A. F., & Bakar, B. (2018). Surface Finish Effects Using Coating Method on 3D Printing (FDM) Parts. *IOP Conference Series, Materials Science & Engineering*, 318, 1.
 - [10] Mwema, F. M., Akinlabi, E. T., & Fatoba, O. S. (2020). Visual assessment of 3D printed elements: A practical quality assessment for home-made FDM products, *Materials Today Proceedings*, (in press).
 - [11] Mwema, F. M. Akinlabi, E. T. & Oladijo, O. P. (2020). Fractal analysis of thin films surfaces: a brief overview, in *Advances in Material Sciences and Engineering. Lecture Notes in Mechanical Engineering*. Springer, Singapore, 251–263.
 - [12] Mwema, F. M., Akinlabi, E. T., & Oladijo, O. P. (2019). Effect of substrate type on the fractal characteristics of AFM images of sputtered aluminium thin films, *Materials Science*, 26(1), 49–57.
 - [13] Ghosh, K., & Pandey, R. K. (2019). Power spectral density-based fractal analysis of annealing effect in low cost solution-processed Al-doped ZnO thin films, *Physica Scripta*, 94(11), 115704.
 - [14] Nečas, D. & Klapetek, P. (2012). Gwyddion: An open-source software for SPM data analysis, *Central European Journal of Physics*, 10(1), 181–188.
 - [15] Korpi, A.G., Talu, S., Bramowicz, M., Arman, A., Kulesza, S., Pszczolkowki, B., Jurecka, S., Mardani, M., Luna, C., Balashabadi, P., Rezaee, S., & Gopikishan, S. (2019). Minkowski functional characterization and fractal analysis of surfaces of titanium nitride films, *Materials Research Express*, 6(8), 086463.
 - [16] Yadav, R. P., Kumar, M., Mittal, A. K., & Pandey, A. C. (2015). Fractal and multifractal characteristics of swift heavy ion induced self-affine nanostructured BaF₂ thin film surfaces, *Chaos: An Interdisciplinary Journal of Nonlinear Science*, 25(8), 083115.
 - [17] Mwema, F. M., Oladijo, O. P., Sathiaraj, T. S. & Akinlabi, E. T. (2018). Atomic force microscopy analysis of surface topography of pure thin aluminium films, *Materials Research Express*, 5(4), 1–15.
 - [18] Mwema, F. M., Akinlabi, E. T., & Oladijo, O. P. (2019). Two-dimensional fast fourier transform analysis of surface microstructures of thin aluminium films prepared by radio-frequency (RF) magnetron sputtering, *Advances in Materials Science & Engineering, Lecture Notes Mechanical Engineering*, Springer, Singapore, 239–249.
 - [19] Mwema, F. M., Akinlabi, E. T., & Oladijo, O. P. (2019). The use of power spectrum density for surface Characterization of Thin Films, *Photoenergy and Thin Film*

Materials, 379–411.

- [20] Arman, A., Țălu, Ș., Luna, C., Ahmadpourian, A., Naseri, M. & Molamohammadi, M. (2015). Micromorphology characterization of copper thin films by AFM and fractal analysis, *Journal of Materials Science: Materials in Electronics*, 26(12), 9630–9639.